Published in final edited form as:
Somatosens Mot Res. 2010 ; 27(1): 34–43. doi:10.3109/08990221003646736.

Organization and morphology of thalamocortical neurons of mouse ventral lateral thalamus

AILEEN P. TLAMSA[1] and **JOSHUA C. BRUMBERG**[2]

[1] Department of Biology, Queens College, CUNY, Flushing, New York, USA

[2] Department of Psychology, Queens College, CUNY, Flushing, New York, USA

Abstract

The ventral lateral nucleus of the thalamus (VL) serves as a central integrative center for motor control, receiving inputs from the cerebellum, striatum, and cortex and projecting to the primary motor cortex. We aimed to determine the somatotopy and morphological features of the thalamocortical neurons within mouse VL. Retrograde tracing studies revealed that whisker-related VL neurons were found relatively anterior and medial to those labeled following injection of retrograde tracer into hindpaw motor areas. Simultaneous injections of fluorescent microspheres in both cortical regions did not result in double-labeled neurons in VL. Quantitative analysis of dendritic and somatic morphologies did not reveal any differences between hindpaw and whisker thalamocortical neurons within VL. The morphology of the thalamocortical neurons within mouse VL is similar to those in other mammals and suggests that mouse can be used as a model system for studying thalamocortical transformations within the motor system as well as plasticity following sensory deprivation or enrichment.

Keywords

thalamus; ventral lateral thalamus; whiskers; somatotopy

Introduction

Primary somatosensory and motor cortices have been widely recognized as somatotopically organized areas of the brain (Woolsey 1958). Although the ascending sensory thalamocortical system has been extensively studied, the motor thalamocortical system is still relatively unknown. Accordingly, efforts have been made to discover the extent to which the motor thalamus and the motor cortex are interrelated. One way to do this is to examine whether the motor thalamus bears a topography relative to the motor map in the cortex.

Amassian and Weiner (1966) found that there are monosynaptic connections between thalamocortical afferents from the ventrolateral (VL) thalamus to the fast pyramidal tract neurons of the primary motor cortex (M1). Moreover, the VL thalamus is dedicated to the relay and feedback of motor information, particularly motor control, as it carries information from the cerebellum (mainly targeting VLp and VPLo; see Table I for abbreviations) and the basal

Correspondence: J.C. Brumberg, PhD, Department of Psychology, Queens College, CUNY, 65–30 Kissena Boulevard, Flushing, NY 11367, USA. Tel: +1 718 997 3541. Fax: +1 718 997 3257. Joshua.brumberg@qc.cuny.edu.

Declaration of interest: The authors report no conflicts of interest. The authors alone are responsible for the content and writing of the paper.

ganglia (mainly targeting VLo) to the motor cortex (Asanuma et al. 1983a; Anner-Baratti et al. 1986; Percheron et al. 1996).

Using retrograde tracing techniques several sub-nuclei have been identified in primate motor thalamus, including VPLo, VPLc, VLc, VLm, VLps, and VLo (see Table I for abbreviations; Olszewski 1938;Strick 1976;Asanuma 1983a;Holsapple et al. 1991). Similar subdivisions have yet to be identified in the rodent. The connections between M1 and VL appear to be reciprocal (Stepniewska et al. 1994;Kakei et al. 2001) and conform to the known motor maps. It is still unclear if each subdivision of VL contains a separate body representation; however, it appears that many of these connections are segregated by their role in motor control (Strick 1976;Stepniewska et al. 1994;Vitek et al. 1994).

In addition to a thalamocortical somatotopic relationship, there is evidence that the cerebello-thalamic pathway is topographically organized as well (Asanuma et al. 1983b). The caudal cerebellum projects to medial thalamus, and the rostral cerebellum projects to lateral thalamus (Schell and Strick 1984; Matelli et al. 1989). Given that the primary inputs to VL are topographic (M1 and cerebellum) it is assumed that VL is also organized in a topographic pattern and describing this organization is the focus of the present paper.

Utilizing retrograde tracers we examined labeling in the VL thalamus after injections into the physiologically verified whisker and hindpaw representations within primary motor cortex. Subsequently, several distinct nuclei were labeled in the motor thalamus. Additionally, we characterized and compared the neuronal morphology of identified thalamocortical relay cells within the whisker and hindpaw representations.

Materials and methods

Animals

All experiments were carried out using CD1 mice of either sex, postnatal day 30–60 (Charles River Laboratories, Wilmington, MA). All experiments were performed in accordance with Queens College's Institutional Animal Care and Use Committee guidelines. The anatomical methods were adapted from those of Johnson and Burkhalter (1997).

Overview

Microstimulation was performed to identify two distinct areas of M1, the regions responsible for whisker movement and hindpaw movement, using a bipolar electrode as previously described (Rocco and Brumberg 2007). Once the areas were confirmed, we injected N-methyl-D-aspartate (NMDA), followed by biotinylated dextran amine (BDA) after a 5-min interval (see below).

Surgical procedures

Mice were anesthetized with ketamine/xylazine (153 mg/kg/2.23 mg/kg) through intraperitoneal (ip) injection. The animals were deemed anesthetized when they became unresponsive to a toe pinch. Each animal was then placed in a small animal stereotaxic apparatus (David Kopf Instruments, Tujunaga, CA). The coordinates for the regions of M1 were based on those of Franklin and Paxinos (1997). A cortical window was made approximately 1 mm × 1 mm over the area of interest. The whisker area was defined around the coordinates 1 mm anterior and 1 mm lateral to bregma. The hindpaw area was defined around the coordinates 1.5 mm posterior and 1.5 mm lateral to bregma. To confirm these locations, a bipolar stimulating electrode (500 μm inter-tip distance, Frederick Hare Co., Brunswick, ME, USA) was inserted perpendicular to the pial surface. The electrode was then inserted to a depth of approximately 300 μm into the cortex. Stimulating pulses were applied

via a stimulus isolation unit (World Precision Instruments, Sarasota, FL), and the pulses were modulated through a Master-8 apparatus (AMPI, Jerusalem, Israel). The stimulation began at a low intensity (0.1 mA) and then gradually increased until a stimulation-evoked movement was observed. The movement of an isolated contralateral whisker or several adjacent whiskers defined the whisker motor area. The movement of the contralateral hindpaw defined the hindpaw motor area. Typically, this movement resulted in the lifting of the hindpaw off of the stereotaxic platform. In no instances were ipsilateral movements of the hindpaw or whiskers evoked and no stimulation sites resulted in simultaneous movement of the whisker pad and hindpaw.

Upon identification of the correct location of the cortical area of interest, an injection of a tracer was made into the area using glass micropipettes (OD/ID in mm; 1.0/0.58) fashioned on a Sutter micropipette puller (P-87, Sutter Instruments, Carlsbad, CA) filled with the appropriate tracers (see below). All injections were performed in the stereotaxic apparatus (Kopf Instruments, Tujunga, CA) while the animal was heavily anesthetized.

NMDA-enhanced BDA labeling

Prior to BDA injection, a precursor injection of NMDA was administered to enhance the retrograde transport of the BDA. First, approximately 0.1 μl of NMDA (10 mM NMDA in 0.01 phosphate buffer (PB), pH 7.0) was injected into the cortical region as previously described (Johnson and Burkhalter 1997). Following a 5-min interval, BDA was injected into the same location (BDA, 2.5 g/ml in 0.001 M phosphate buffer saline (PBS, Carlsbad, CA); Molecular Probes).

NMDA–BDA was either injected using pressure injection (Toohey IIe, Toohey Company, Fairfield, NJ) into the appropriate region of M1 using pulses of pressurized N_2 (duration<1.0 ms) or via a Hamilton syringe. No difference in retrograde transport was seen between the two different injection methods, both areas resulted in the same areas being labeled. Animals survived for at least 2 days to allow for adequate transport time.

Bead injections

In order to quantify potential overlap between whisker and hindpaw representations within the VL thalamus, fluorescent beads were simultaneously injected into the physiologically identified whisker and hindpaw representations of M1 as previously described (Rocco and Brumberg 2007). Two types of beads were utilized, green beads (FITC conjugated) and red beads (rhodamine conjugated, both from Lumaflour Inc., Raleigh, NC). One type (color) was injected into each interest area of the motor cortex. For instance, M1-whisker received green beads and M1-hindpaw would receive red beads, and vice versa. Two animals received green beads in the whisker representation of M1 and red beads in the hindpaw representation and two animals received red bead injections in the whisker region and green beads in the hindpaw representation of M1.

Animals survived 3–4 days to allow for adequate transport of the beads and then perfused as above and slices were cut on a Vibratome at 50 μm and incubated in 0.1 PBS overnight. Every other slice was taken for fluorescent use, and the remaining slices were kept for Nissl stain. The intended slices were then dehydrated and mounted. A fluorescent mounting media (Vectashield, Vector Laboratories, Burlingame, CA) was used to preserve the beads' fluorescent intensity. Slides were kept refrigerated (4°C) and kept in the dark. Slices were observed under the Olympus Bx51 microscope using a Hg-lamp fluorescent light source and appropriate excitation and emission filters.

Tissue preparation

Mice were anesthetized through an ip injection of nembutal (0.1 mg/100 g) and perfused with 0.9% saline followed by 4% paraformaldehyde in 0.1 M PB. Tissue was postfixed overnight in 4% paraformaldehyde in 0.1 M PB. Coronal sections (50 μm) containing M1 and thalamus were obtained using a Vibratome (Ted Pella Inc., Redding, CA). Slices were alternatively processed for BDA or Nissl as previously described (Rocco and Brumberg 2007; Ramos et al. 2008).

BDA was revealed with 3,3′-diaminobenzidine (DAB) using a staining protocol adapted from previously published protocols (Rocco and Brumberg 2007; Ramos et al. 2008). Free floating 50 μm sections were bathed in 0.1 M cold PBS, 3 × 10 min. A 2 × 10-min wash of 0.1 M PB was given, followed by a 30-min wash of 0.1% H_2O_2 and 0.01% methanol. The slices were then bathed again in 0.1 M PB and incubated (2 × 30 min) in a blocking solution of 0.1 M PBS, 0.4% Triton-X (Sigma, St. Louis, MO), and 0.5 mg/ml bovine serum albumin (BSA, Fisher Scientific, Pittsburgh, PA). The slices were then incubated overnight in an avidin–biotin–peroxidase complex (ABC kit, Vector Laboratories) and kept at 4°C overnight.

The slices were then rinsed (4 × 10 min) in 0.1 M PBS at room temperature, incubated in a DAB/NAS solution (5 mg/ml in 0.1 M PB; 0.5% H_2O_2 and nickel ammonium sulfate (NAS), 1.10 g/10 ml H_2O), and shaken lightly (on an orbital shaker). Hydrogen peroxide was then added to the solution and shaken lightly. Upon visualization of a brown/black precipitate, sections were removed from the DAB solution and transferred into 0.1 M PBS and washed (4 × 10 min). Slices were then mounted, dehydrated, and defatted. Slides were coverslipped with DPX mounting media.

Data analyses

Mounted sections were viewed with an Olympus BX51 microscope using 4× (0.1 NA), 10× (0.4 NA), and 60× (1.4 NA, oil immersion) objectives. Digital images were taken with an Optronics Microfire camera attached to a dedicated PC via firewire connection.

Brain slices were traced using the Neurolucida (Microbrightfield Inc., Williston, VT) program in Serial Section Manager. With each slice viewed, the pia matter was traced, following a trace of white matter, and injection site (at 4×). Cells filled with the NMDA–BDA were then indicated with markers in both the motor cortex and the thalamus. Using serial sections, a three-dimensional view of the marked cells in cortex and thalamus can be viewed. Retrogradely labeled VL neurons of interest were traced (Neurolucida) and analyzed (Neuroexplorer, Microbrightfield Inc.) as previously described (Chen et al. 2009). Tracing was performed at 60× (1.4 NA) magnification. Several dendritic and somatic morphological parameters were quantified for comparison between completely reconstructed neurons. Somatic metrics included cell body area and perimeter, Ferret Maximum, which refers to the longest diameter of the soma, and Ferret Minimum which is the longest diameter perpendicular to the Ferret Maximum and their ratio was used to compute the cell's aspect ratio (Ferret Maximum/Ferret Minimum). As a cell's aspect ratio approaches one, it is indicative that the soma is closer to a symmetric shape (e.g., circle or square). Total dendritic length as well as the number of primary, secondary, and tertiary neurons was quantified. To compare dendritic architecture a Sholl analysis was conducted in which the cell body was placed at the center of concentric circles (with diameters incrementing by 10 μm) and the number of intersections per annulus as well as the length and number of dendritic nodes contained within each circle were quantified. Neuronal metrics were compared using ANOVAs and Tukey's post-hoc tests (Statistica) and an alpha value of $p<0.05$ was used as a criterion of statistical significance. Data are presented as mean ± 1 standard error of the mean unless otherwise noted.

Results

Distinct thalamic representations

The whisker and hindpaw representations in the mouse motor cortex were chosen for this study. These two areas were chosen because each encompasses a large dedicated region in the mouse motor cortex, and the two areas are anatomically separated on the cortical surface by about 2 mm (Franklin and Paxinos 1997). This spacing would minimize the probability of overlap of the injected tracers within the motor cortex.

Following injections of NMDA–BDA into the whisker and hindpaw representations of M1 several subdivisions within the motor thalamus were labeled. Transport from M1 to ipsilateral thalamus was observed in all animals (n = 10 of 10). Similar patterns of labeling were observed in the ipsilateral motor thalamus in all animals with similar target injection areas (i.e., vibrissae or hindpaw). Labeled cells were also observed at the injection site in M1. Larger injections revealed labeling of the callosum, and thus labeled cells in the secondary somatosensory and motor cortices of the contralateral hemisphere. The cells labeled after M1-whisker injections mainly occupied the VL proper and the laterodorsal dorsomedial thalamus (LDDM), (Figure 1B). The cells labeled after M1-hindpaw injections mainly occupied the ventral posterior lateral nucleus (VPL), VL, and the laterodorsal ventrolateral thalamus (LDVL) thalamic nuclei as well as nRT (Figure 1C). In sum, the neurons labeled following whisker M1 injections were found anterior and medial to those following hindpaw injections.

Characterization of VL subdivisions

Previous studies of motor thalamus have shown specific topographies in the monkey (Holsapple et al. 1991; Stepniewska et al. 1994; Vitek et al. 1994). Our study sought to expand these findings to the rodent model. Distinctly different areas of the VL thalamus were labeled following injections into either M1 hindpaw or vibrissa regions. Following injections of NMDA–BDA into the M1 area responsible for vibrissae movement, the most densely stained thalamic nucleus was the VL proper, with fewer retrogradely filled neurons in LDDM, Po, LPMR (lateropostero mediorostral), and VPL (Franklin and Paxinos 1997). Following injections of NMDA–BDA into the M1 area responsible for hindpaw movement, the most densely labeled thalamic area was the LDVL, with less dense labeling evident in LPLR (lateropostero laterorostral) and VPL (Franklin and Paxinos 1997, see Figures 1 and 2). We identified the thalamic location of each labeled cell body following injections in the hindpaw and whisker regions of M1 (representative sections are shown in Figure 2A, B). Upon overlaying the sections (from different animals) the relative positions of the hindpaw and whisker representations were evident, with the hindpaw located more lateral and dorsal relative to the whisker region.

To determine whether neurons in the thalamus projected to both whisker and hindpaw regions of M1 rhodamine-labeled beads or fluorescein-labeled beads were injected into both representations within the same animal. The retrogradely labeled areas following these experiments were identical to those following the BDA injections. Labeling was seen in respective VLs of whisker and hindpaw; however, double-labeled neurons within the VL were never observed (n = 4). The labeling was similar to that seen in Figure 2B, C. Thus as in M1 the whisker and hindpaw representations within the thalamus appear to be non-overlapping.

Characterization of thalamocortical neurons within whisker and hindpaw VL

Previous studies in the human, monkey, and rodent have qualitatively identified different neuronal cell types within the motor thalamus (Sawyer et al. 1989; Berezhnaya 2003). There are a large variety of cell types within the thalamus, and still within the motor thalamus there is great variation as well. Cell types have previously been qualitatively identified by their size,

the degree of staining of the cytoplasm and the nucleus, the neuronal shape, and most importantly, the branching (e.g., Sawyer et al. 1989; Berezhnaya 2003), but few studies have focused on identified thalamocortical projection neurons.

Within the labeled VL areas for both whisker and hindpaw injections, neurons that appeared to be completely filled were observed using a 60× objective (oil immersion, 1.4 NA), neurons with ovoid cell bodies that possessed dendrites that tapered to a point were selected for tracing using Neurolucida (see Methods, Figure 3). This allowed us to reconstruct a relatively homogeneous population of thalamocortical relay cells.

Retrogradely labeled thalamocortical projection neurons within VL were characterized by oval cell bodies and multipolar dendritic trees. Characteristic of oval cell bodies, the Ferret Maximum was larger than the Ferret Minimum (Table II) which resulted in aspect ratios of 1.47 ± 0.12 and 1.38 ± 0.06 *for neurons backfilled from whisker and hindpaw M1 areas*, respectively. The neurons within whisker VL ($n = 11$) had an average somal area of 194.62 ± 15.7 μm^2 whereas the neurons within hindpaw VL ($n = 11$) had an average somal area of 174.84 ± 15.2 μm^2. Statistical comparisons of the somatic variables revealed no differences between the labeled neurons within the two representations within VL and thus their data was pooled and is represented in Table II.

The branching of dendritic arbors of the two groups was also compared (Table II, Figure 4). The average number of primary dendrites for whisker VL neurons was 4.00 ± 0.40 and hindpaw VL neurons possessed and average of 4.55 ± 0.37 primary dendrites. Both groups had similar numbers of secondary and tertiary dendrites (Table III). The neurons did not differ in their total dendritic length, whisker VL relay cells had an average length of their dendritic arbors of 672.51 ± 117.01 μm and the relay neurons in the hindpaw representation had an average dendritic length of 816.32 ± 126.22 μm.

Although the VL relay neurons had similar lengths and number of dendrites it is possible that they had different architectures. To further look at this issue we performed a Sholl analysis wherein the soma is placed in the center of a series of concentric circles (each 10 μm larger in diameter) which allows for the assessment of dendritic architecture by counting the number of dendritic intersections as a function of distance from the soma. For both groups, number of intersections, dendritic length (μm), and dendritic nodes were plotted against the distance from the soma. The patterns for all three variables were not statistically different between whisker and hindpaw cells ($p \geq 0.05$, see Figure 5).

Thus, based on quantitative reconstruction and statistical comparisons of the somatic and dendritic variables of the whisker and hindpaw VL neurons, it appears that VL relay neurons constitute a homogeneous morphological group.

Discussion

Previous studies in humans and primates have displayed topographic specificity within the motor thalamus (Strick 1976; Holsapple et al. 1991; Stepniewska et al. 1994; Vitek et al. 1994) and VL inputs to different motor representations in the motor cortex appear to be separated by functional representation of different muscle groups/body parts. With the increased utilization of mouse models, due largely to the advances in genetic technologies it is becoming increasingly important to characterize baseline circuits in order to understand how their degradation/dysfunction can result in neural pathologies. The present study observed topographic separation of the VL inputs to the motor cortex within the mouse, similar to previous findings in humans and primates (Holsapple et al. 1991; Stepniewska et al. 1994; Vitek et al. 1994). This suggests that different muscle groups are regulated by distinct regions of the thalamus. Those areas dedicated to the medial muscles, such as the whisker pad, were

found to be more medial and posterior in the mouse motor thalamus. The hindpaw area, like more lateral musculature, was more lateral in the thalamus. Within the primate VL there is a fine scale organization of the motor map with subregions of the arm and hand being represented by distinct clusters of cells (Strick 1976), our level of analysis did not allow us to see if there was a row or arc-like representation of the whisker within VL.

The topographic organization of the rodent motor thalamus is consistent with the findings in the primate and cat (Shinoda et al. 1993a; Morel et al. 2005), and the thalamic map represents a site of convergence of homotopic descending corticothalamic inputs from M1 (Kakei et al. 2001) as well as from other premotor areas (Morel et al. 2005) and ascending cerebellar inputs (Shinoda et al. 1993b; Holsapple et al. 1991). The motor thalamus is not the only recipient of these cerebellar inputs and in turn VL does not give rise to all the thalamic input into the motor cortex (Strick 1975; Huffman and Krubitzer 2001), but it is likely that homotopic representations in other thalamic nuclei that project to M1 such as POM and VPL project convergently to similar cortical areas. Although the thalamic nuclei may differ from the rodent and the primate, the organization and pathways of the two motor systems appear highly synonymous.

Methodological considerations

We targeted physiologically confirmed regions of M1 with injections of NMDA and BDA (Jiang et al. 1993; Johnson and Burkhalter 1997; Di Rocco et al. 2001). This method of retrograde tracing is reliable and provides a well-defined preservation of ultra-structure, displaying organization of circuits (Jiang et al. 1993; Johnson and Burkhalter 1997). The thalamic neurons retrogradely labeled were found in nuclei previously associated with motor planning and the execution of modulation of ongoing motor activities, and similar nuclei were identified following use of fluorescent latex microspheres confirming the efficacy of the technique.

Thalamocortical relay neurons comprise a homogeneous morphological group

In the present study only thalamocortical relay neurons were identified and comparisons of neuronal morphology between whisker and hindpaw VL revealed no significant differences. The morphological similarity in these two groups of thalamocortical neurons suggests they may play similar functional roles. Within the visual system of cats and primates thalamocortical neurons can be subdivided based on their functional classifications into three distinct classes, each with a relatively distinct soma size and dendritic architecture (Friedlander et al. 1981). Such distinctions were not apparent in our VL dataset. Similar distinctions are present in the rat auditory system where thalamocortical neurons projecting to different areas of the primary auditory cortex have different morphologies (Winer et al. 1999). However, within the somatosensory system, thalamocortical neurons of the ventral posterior medial nucleus which processes whisker information (Chiaia et al. 1991; Brecht and Sakmann 2002) and the ventral posterior lateral nucleus which processes information from the rest of the body including the hindlimb (Ohara et al. 1995) have similar morphologies. This finding is consistent with our findings in VL as the thalmocortical relay cells in the whisker and hindpaw representations had indistinguishable morphologies. Overall the differences between the different thalamocortical relay neurons are relatively small and suggest that the morphology of these neurons is likely well adapted to their role in recurrent thalamocortical circuits.

Acknowledgments

Thanks to Drs Raddy L. Ramos and Carolyn Pytte for help with labeling and comments on the manuscript. The work was funded by NS058758-02.

References

Amassian, V.; Weiner, H. Monosynaptic and polysynaptic activation of pyramidal tract neurons by thalamic stimulation. The thalamus. New York: Columbia University Press; 1966. p. 255-282.

Anner-Baratti RE, Allum HJ, Hepp-Raymond MC. Neural correlates of isometric force in the "motor" thalamus. Exp Brain Res 1986;63:567–580. [PubMed: 3758268]

Asanuma C, Thach TW, Jones E. Cytoarchitectonic delineation of the ventral lateral thalamic region in the monkey. Brain Res 1983a;286(3):219–235. [PubMed: 6850357]

Asanuma C, Thach TW, Jones E. Distribution of cerebellar terminations and their relation to the other afferent terminations in the ventral lateral thalamic region of the monkey. Brain Res Rev 1983b;5:237–265.

Berezhnaya LA. Neuronal organization of the ventral anterior and ventral lateral nuclei of the human thalamus. Neurosci Behav Physiol 2003;33(4):357–362. [PubMed: 12774837]

Brecht M, Sakmann B. Whisker maps of neuronal subclasses of the rat ventral posterior medial thalamus, identified by whole-cell voltage recording and morphological reconstruction. J Physiol 2002;538:495–515. [PubMed: 11790815]

Chen C-C, Abrams S, Pinhas A, Brumberg JC. Morphological heterogeneity of layer VI neurons in mouse barrel cortex. J Comp Neurol 2009;512(6):726–746. [PubMed: 19065632]

Chiaia NL, Rhoades RW, Fish SE, Killackey HP. Thalamic processing of vibrissal information in the rat: II. Morphological and functional properties of medial ventral posterior nucleus and posterior nucleus neurons. J Comp Neurol 1991;314:217–236. [PubMed: 1723993]

Di Rocco F, Giannetti S, Gaglini P, Di Rocco C, Granato A. Dendritic anomalies in a freezing model of microgyria: A parametric study. Pediatr Neurosurg 2001;34(2):57–62. [PubMed: 11287804]

Franklin, KBJ.; Paxinos, G. The mouse brain in stereotaxic coordinates. San Diego: Academic Press; 1997.

Friedlander MJ, Lin CS, Stanford LR, Sherman SM. Morphology of functionally identified neurons in lateral geniculate nucleus of the cat. J Neurophysiol 1981;46(1):80–129. [PubMed: 7264710]

Holsapple J, Preston J, Strick P. The origin of thalamic inputs to the "hand" representation in the primary motor cortex. J Neurosci 1991;11(9):2644–2654. [PubMed: 1715388]

Huffman KJ, Krubitzer L. Thalamo-cortical connections of areas 3a and M1 in marmoset monkeys. J Comp Neurol 2001;435(3):291–310. [PubMed: 11406813]

Jiang X, Johnson RR, Burkhalter A. Visualization of dendritic morphology of cortical projection neurons by retrograde axonal tracing. J Neurosci Methods 1993;50:45–60. [PubMed: 7506340]

Johnson R, Burkhalter A. A polysynaptic feedback circuit in rat visual cortex. J Neurosci 1997;17(18): 7129–7140. [PubMed: 9278547]

Kakei S, Na J, Shinoda Y. Thalamic terminal morphology and distribution of single corticothalamic axons originating from layers 5 and 6 of the cat motor cortex. J Comp Neurol 2001;437:170–185. [PubMed: 11494250]

Matelli M, Luppino G, Fogassi L, Rizzolatti G. Thalamic input to inferior area 6 and area 4 in the macaque monkey. J Comp Neurol 1989;280:468–488. [PubMed: 2537345]

Morel A, Liu J, Wannier T, Jeanmonod D, Rouiller EM. Divergence and convergence of thalamocortical projections to premotor and supplementary motor cortex: A multiple tracing study in the macaque monkey. Eur J Neurosci 2005;21(4):1007–1029. [PubMed: 15787707]

Ohara PT, Ralston HJ 3rd, Havton LA. Architecture of individual dendrites from intracellularly labeled thalamo-cortical projection neurons in the ventral posterolateral and ventral posteromedial nuclei of cat. J Comp Neurol 1995;358:563–572. [PubMed: 7593750]

Olszewski, J. The primate thalamus. Chicago: University of Chicago Press; 1938.

Paxinos, G.; Franklin, KBJ. The mouse brain in stereotaxic coordinates. 2. San Diego: Academic Press; 2001.

Percheron G, François C, Talbi B, Yelnik J, Fénelon G. The primate motor thalamus. Brain Res Rev 1996;22:93–181. [PubMed: 8883918]

Ramos RL, Tam D, Brumberg JC. Physiology and morphology of callosal projection neurons in mouse. Neuroscience 2008;153(3):654–663. [PubMed: 18424008]

Rocco MM, Brumberg JC. The sensorimotor slice. J Neurosci Methods 2007;162:139–147. [PubMed: 17307257]

Sawyer S, Young S, Groves P. Quantitative Golgi study of anatomically identified subdivisions of motor thalamus in the rat. J Comp Neurol 1989;286(1):1–27. [PubMed: 2475532]

Schell G, Strick P. The origin of thalamic inputs to the arcuate premotor and supplementary motor areas. J Neurosci 1984;4:539–560. [PubMed: 6199485]

Shinoda, Y.; Futami, T.; Kakei, S. Input–output organization of the ventrolateral nucleus of the thalamus. Proceedings of the 2nd International Workshop on Microphysiological Recordings during Stereotactic Neurosurgery: Motor Thalamus; 1993a. p. 17-31.

Shinoda Y, Kakei S, Futami T, Wannier T. Thalamocortical organization in the cerebello-thalamo-cortical system. Cereb Cortex 1993b;3:421–429. [PubMed: 8260810]

Stepniewska I, Preuss T, Kaas JH. Thalamic connections of the primary motor cortex (M1) of owl monkeys. J Comp Neurol 1994;349:558–582. [PubMed: 7532193]

Strick PL. Multiple sources of thalamic input to the primate motor cortex. Brain Res 1975;88(2):372–377. [PubMed: 50113]

Strick P. Anatomical analysis of ventrolateral thalamic input to primate motor cortex. J Neurophys 1976;39(5):1020–1031.

Vitek JL, Ashe J, DeLong MR, Alexander GE. Physiologic properties and somatotopic organization of primate motor thalamus. J Neurophys 1994;71(4):1498–1513.

Winer JA, Sally SL, Larue DT, Kelly JB. Origins of medial geniculate body projections to physiologically defined zones of rat primary auditory cortex. Hear Res 1999;130(1–2):42–61. [PubMed: 10320098]

Woolsey, CN. Biological and biochemical basis of behavior. Madison: University of Wisconsin Press; 1958. Organization of somatic sensory and motor areas of the cerebral cortex; p. 63-81.

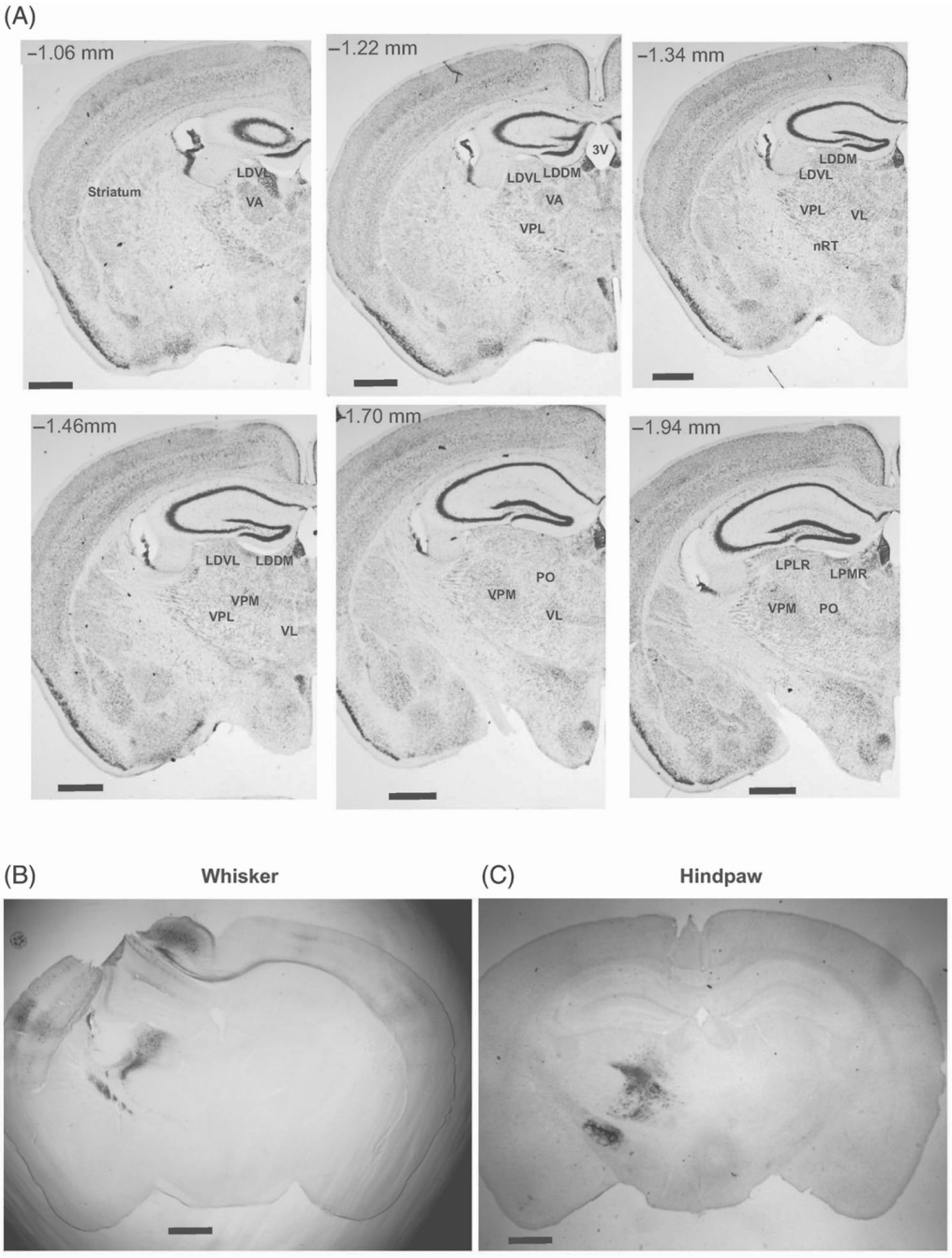

Figure 1.

Representative VL labeling following cortical injections. Representative Nissl stained coronal sections with thalamic motor nuclei identified, abbreviations as in Table I, numbers indicate relative position relative to bregma (Paxinos and Franklin 2001). Labeling following whisker (B) vs. hindpaw (C) identified different regions within VL. Scale bars represent 1 mm.

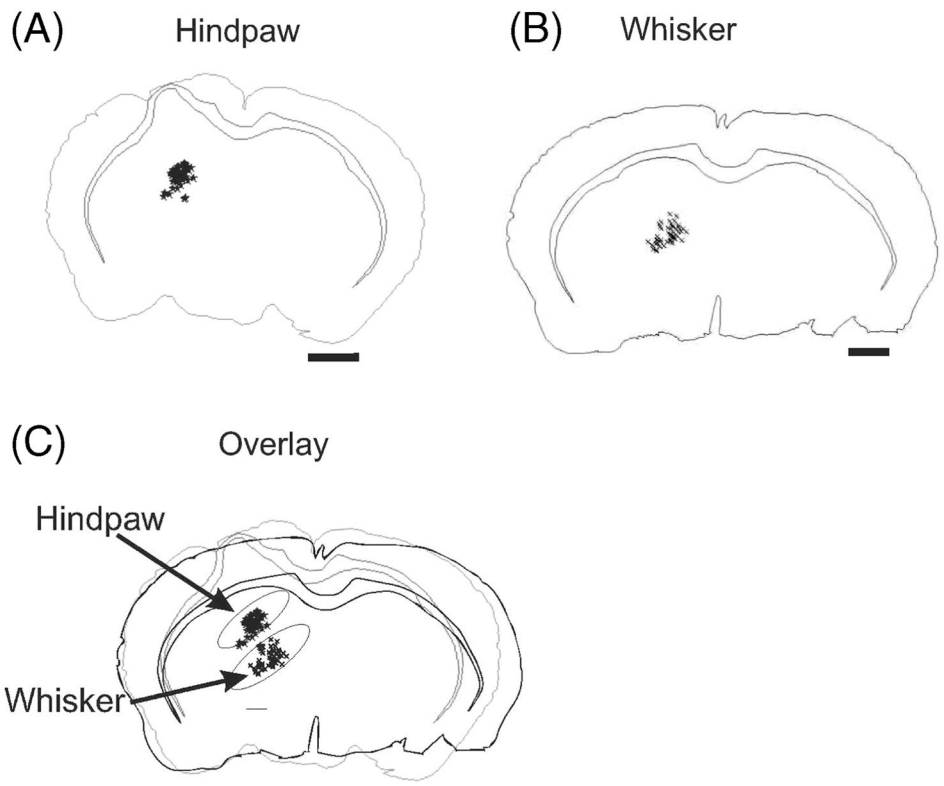

Figure 2.

Localization of labeled neurons within VL. Representative coronal sections from VL. Neurons were labeled laterally and more dorsally following hindpaw injections in M1 (A) in comparison to whisker injections in a different animal which resulted in labeling of more medial VL (B). The largely non-overlapping representations are observed in the overlay (C). Scale bars represent 1 mm.

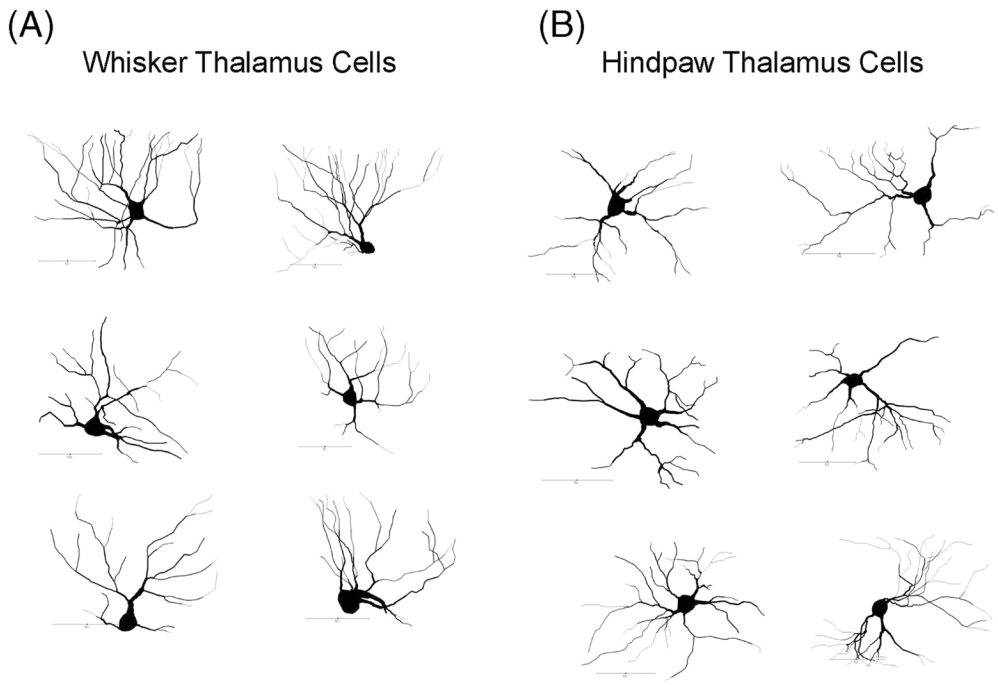

Figure 3.
Neurolucida neuronal reconstructions. Two-dimensional representations of reconstructed whisker (A) and hindpaw (B) neurons. All neurons are oriented such that dorsal is towards the top of the figure. Scale bars represent 50 μm.

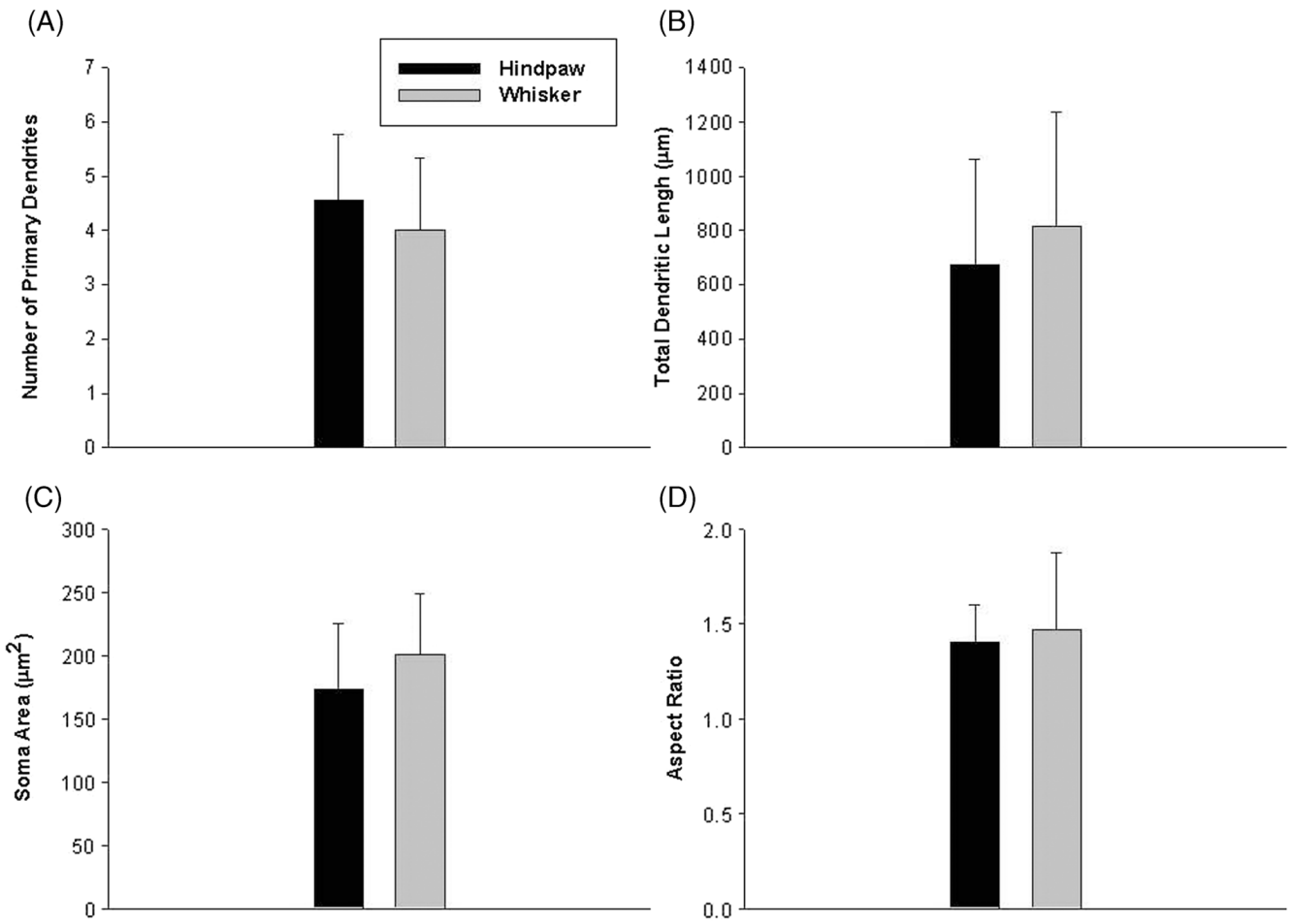

Figure 4.

Morphological characteristics of VL neurons. The number of primary dendrites did not differ between hindpaw (black) and whisker (gray) projection VL neurons (A) nor did the total dendritic length (B). The somas of the two populations of projection neurons had similar areas (C) and aspect ratios (D). Bars represent means ± 1 standard deviation.

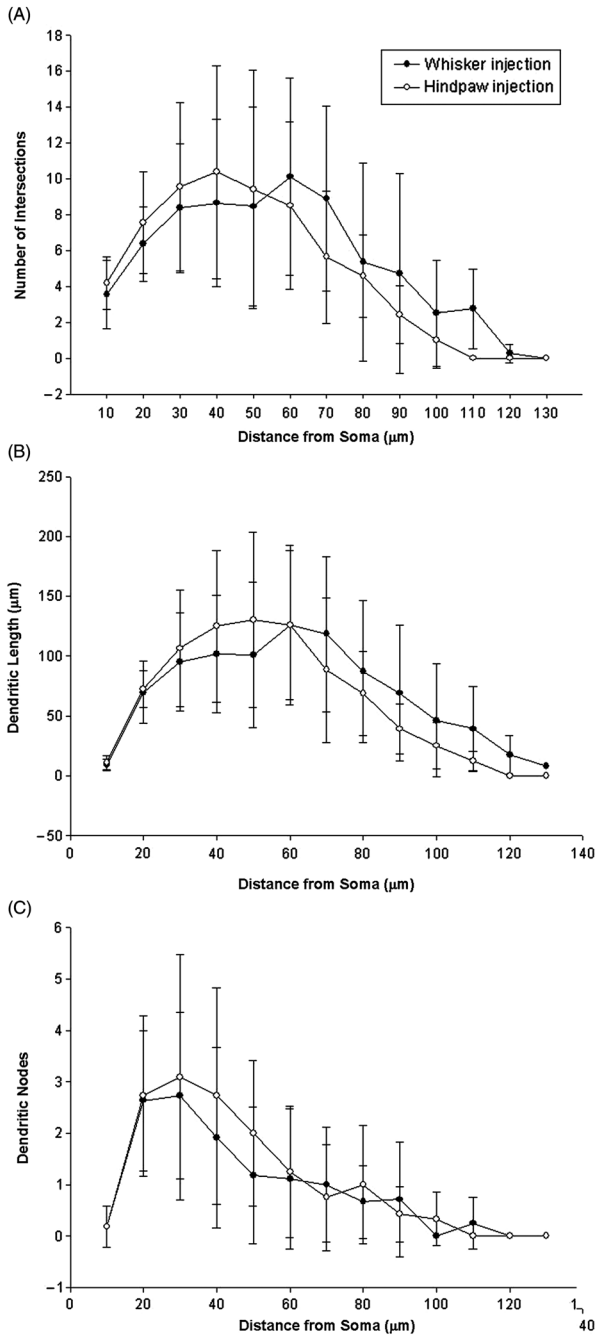

Figure 5.

Sholl analysis of VL neurons. Analysis of number of dendritic intersections (A), dendritic length within each concentric circle (B), and the number of nodes (C) reveal no difference between neurons projecting to whisker M1 (black circles) vs. hindpaw M1 (open circles). Means ±1 standard deviation are plotted.

Table I

Abbreviations of thalamic nuclei.

3V	Third ventricle
LDVL	Laterodorsal ventrolateral nucleus of thalamus
LDDM	Laterodorsal dorsomedial nucleus of thalamus
LPMR	Lateropostero mediorostral nucleus of thalamus
LPLR	Lateropostero laterorostral nucleus of thalamus
nRT	Nucleus reticularis of the thalamus
PO	Posterior nucleus of thalamus
VA	Nucleus ventralis anterior
VApc	Nucleus ventralis anterior pars parvocellularis
VLa	Nucleus ventralis lateralis anterior
VL	Nucleus ventralis lateralis
VLc	Nucleus ventralis lateralis pars caudalis
VLd	Nucleus ventralis lateralis dorsalis
VLm	Nucleus ventralis lateralis pars medialis
VLo	Nucleus ventralis lateralis pars oralis
VLp	Nucleus ventralis lateralis posterior
VLps	Nucleus ventralis lateralis pars postrema
VPLo	Nucleus ventralis posterior lateralis pars oralis
VPLc	Nucleus ventralis posterior lateralis pars caudalis

Table II

Somatic measurement of VL neurons: data presented as means ± 1 standard error of the mean.

Variable	Hindpaw (*n* = 11)	Whisker (*n* = 11)	Combined (*n* = 22)
Perimeter (μm)	49.53 ± 2.7	53.37 ± 2.48	51.45 ± 1.89
Area (μm^2)	174.84 ± 15.19	194.62 ± 15.67	184.73 ± 10.87
Ferret max (μm)	17.86 ± 1.12	19.68 ± 1.17	18.77 ± 0.81
Ferret min (μm)	12.95 ± 0.57	13.67 ± 0.71	13.31 ± 0.45
Aspect ratio	1.38 ± 0.06	1.47 ± 0.12	1.42 ± 0.31

Table III

Dendritic measurement of VL neurons: data presented as means ± 1 standard error of the mean.

Variable	Hindpaw (*n* = 11)	Whisker (*n* = 11)	Combined (*n* = 22)
Primary dendrites	4.00 ± 0.40	4.55 ± 0.37	4.27 ± 0.27
Secondary dendrites	8.00 ± 0.86	7.81 ± 1.03	7.91 ± 0.66
Tertiary dendrites	8.30 ± 1.28	9.00 ± 1.20	8.65 ± 0.86
Total dendritic length (μm)	816.32 ± 126.22	672.51 ± 117.01	744.41 ± 85.44